

Contents

Table of Contents	1
1 Introduction	2
2 Background	3
3 Smooth	6
3.1 Projections from 3-manifolds to \mathbb{R}^2	7
3.2 Stratifying \mathbb{R}^2	9
3.3 Stratifying M	11
3.4 Attach Handles	19
3.4.1 2-handles	19
3.4.2 3-handles	22
3.4.3 4-handles	24
4 Triangulated	25
4.1 Define projection	26
4.2 Induce subdivision	28
4.3 Attach Handles	31
4.3.1 Attach 2-handles	31
4.3.2 Attach 3-handles	33
5 Conclusion	34
Bibliography	35

Chapter 1

Introduction

The main goal of this document is to provide an algorithm whose input is a closed, orientable 3-manifold triangulation M and whose output is a 4-manifold triangulation whose boundary is M . This algorithm mirrors the constructive proof that a smooth, closed, orientable 3-manifold bounds some 4-manifold presented in Chapter 3.

Chapter 2

How do you obtain a 4–manifold with a specific boundary?

Given a smooth, closed 3–manifold M , there are infinitely many 4–manifolds with boundary M . We do not ensure that the constructed 4–manifold has any properties other than a specified boundary, so our construction ensures easy verification that the constructed 4–manifold’s boundary is exactly M . This is done by setting $W = M \times [0, 1]$, so W has boundary

$$\partial W = (M \times \{0\}) \cup (M \times \{1\}) = M_0 \cup M_1.$$

We then attach stratified handles to the boundary of W away from M_0 until only M_0 remains.

The concept of a stratified handle attachment needs some explanation. First, we define attachment of topological spaces, and use that language to define handle attachment.

Definition 2.0.1 (Attachment). Let X and Y be topological spaces, $A \subset X$ a subspace, and $f : A \rightarrow Y$ a continuous map. We define a relation \sim by putting $f(x) \sim x$ for every x in A . Denote the quotient space $X \sqcup Y / \sim$ by $X \cup_f Y$. We call the map f the *attaching map*. We say that X is *attached* or *glued* to Y over A . A space obtained through attachment is called an *adjunction space* or *attachment space*.

Alternatively, we let A be a topological space and let $i_X : A \rightarrow X$, $i_Y : A \rightarrow Y$ be inclusions. Here, the adjunction is formed by taking $i_X(a) \sim i_Y(a)$ for every $a \in A$ and we denote the adjunction space by $X \cup_A Y$.

Definition 2.0.2 (Handle). Take $n = \lambda + \mu$ and M a smooth n -manifold with nonempty boundary ∂M . Let D^λ be the closed λ -disk and put $H^\lambda = D^\lambda \times D^\mu$. Let $\varphi : \partial D^\lambda \times D^\mu \rightarrow \partial M$ be an embedding and an attaching map between M and H^λ . The attached space H^λ is an n -dimensional λ -handle, and $M \cup_\varphi H^\lambda$ is the result of an n -dimensional λ -handle attachment.

Handle attachment is defined for smooth manifolds, but the resulting attachment space is not a smooth manifold. Rather, the result is a stratified manifold. We use the definition from [5].

Definition 2.0.3 (Stratification). X is a *filtered space* on a finite partially ordered indexing set S if

1. there is a closed subset X_s for each $s \in S$,
2. $s \leq s'$ implies that $X_s \subset X_{s'}$, and
3. the inclusions $X_s \hookrightarrow X_{s'}$ satisfy the homotopy lifting property.

The X_s are the *closed strata* of X , and the differences

$$X^s = X_s \setminus \bigcup_{r < s} X_r$$

are *pure strata*.

A *filtered map* between spaces filtered over the same indexing set is a continuous function $f : X \rightarrow Y$ such that $f(X_s) \subset Y_s$, and such a map is *stratified* if $f(X^s) \subset Y^s$. This leads to definitions of stratified homotopy, therefore stratified homotopy equivalence.

Immediate examples of stratified manifolds are manifolds with boundary and manifolds with corners. Many handles (e.g. $[0, 1] \times [0, 1]$) are manifolds with corners, and the result of a smooth handle attachment is a manifold with corners at $\varphi(\partial D^\lambda \times \partial D^\mu)$. Hence both are stratified manifolds.

A *stratified handle attachment* is a handle attachment where the handle, the manifold to which we attach the handle, and the attaching map are each stratified. The main distinctions between stratified handle attachment and handle attachment are:

1. the handle is necessarily stratified, though the stratification is not necessarily induced by the corners that occur in the standard formation of a handle as the Cartesian product of a pair of disks,

2. the manifold to which we attach the handle is necessarily stratified, and
3. the attaching map ensures that there is a coherent identification between the strata of the handle and the strata of the manifold (i.e. the stratification of the resulting attachment space is well-defined).

Chapter 3

Constructive proof that a smooth, closed, orientable 3–manifold is the boundary of some 4–manifold

We prove that every smooth, closed, orientable 3–manifold is the boundary of some 4–manifold. We do so by explicitly constructing such a 4–manifold from a given 3–manifold. This construction is mirrored in Chapter 4 where we prove the same for a given closed, orientable 3–manifold triangulation and provide an algorithm.

Let M be a smooth, closed, orientable 3–manifold and take $W = M \times [0, 1]$. Then W is a 4–manifold with boundary

$$\partial W = (M \times \{0\}) \cup (M \times \{1\}) = M_0 \cup M_1.$$

We construct a manifold with only one boundary component from W by attaching 4–dimensional 2–, 3–, and 4–handles to W over the part of its boundary away from M_0 . We start by attaching 2–handles to W over M_1 to produce a 4–manifold W' with boundary $M_0 \sqcup M'_1$, where $M'_1 = \partial W' \setminus M_0$ and is described via surgery on M_1 . We then attach 3–handles to W' over M'_1 to produce a 4–manifold W'' with boundary $M_0 \sqcup M''_1$. As before, $M''_1 = \partial W'' \setminus M_1$ and M''_1 is described via surgery on M'_1 . At this point in the construction, M''_1 is the disjoint union of a finite number of copies of S^3 . We attach 4–handles to W'' over M''_1 to produce a 4–manifold whose boundary is exactly M_0 .

Instructions for handle attachment come from defining a projection $f : M_1 \rightarrow \mathbb{R}^2$ that induces a stratification of $M_1 \subset \partial W$.

We call a closed 3-dimensional stratum of M_1 a *block*, and we impose conditions on f to ensure that every block can be classified up to *stratified homeomorphism*. We say that X, Y are *stratified homeomorphic* if X, Y are stratified spaces and there exists a homeomorphism $f : X \rightarrow Y$ such that f and f^{-1} are each stratified maps. The blocks of M_1 are described below:

- *face block*: An attachment neighbourhood for a stratified 2-handle. Each face block is stratified-homeomorphic to $S^1 \times G_n$, the product of the circle with an n -gon for some n .
- *edge block*: A partial attachment neighbourhood for a stratified 3-handle. Each edge block is stratified-homeomorphic to one of $D^2 \times [0, 1]$, $A \times [0, 1]$, or $P \times [0, 1]$, where A is the annulus $S^1 \times [0, 1]$ and P is a pair-of-pants surface. Attachment of stratified 2-handles over our face blocks “fill in” the annular boundary components of edge blocks, forming full attachment neighbourhoods for stratified 3-handles.
- *vertex block*: A partial attachment neighbourhood for a stratified 4-handle. Each vertex block is homeomorphic to a (3,1)-handlebody of genus at most 3. When stratified 2- and 3-handles are attached to W , the genus of these handlebodies are reduced until the remaining boundary of W consists of M_0 union a collection of stratified 3-spheres. The 3-spheres are then coned away.

The remainder of this chapter is spent ensuring that such a stratification can be achieved for any smooth, orientable, closed 3-manifold, detailing how the stratification is induced, proving that the attachment of stratified 2- and 3-handles has the previously stated effects, and discussing the resulting 4-manifold.

3.1 Projections from 3-manifolds to \mathbb{R}^2

Our stratification of M is induced by a decomposition of the plane, itself induced by the singular values of a smooth map $M \rightarrow \mathbb{R}^2$. To prove that a stratification suitable for our construction exists for any smooth orientable 3-manifold, we show first that an inducing decomposition of \mathbb{R}^2 exists. To prove that such a decomposition of \mathbb{R}^2 exists, we present the properties of $f : M \rightarrow \mathbb{R}^2$ required to induce the decomposition, and argue why a map possessing such properties exists for any smooth, orientable 3-manifold.

Let $f : M \rightarrow \mathbb{R}^2$ be a smooth map, let df be the differential of f , and let $S_r(f)$ be the set of points in M such that df has rank r . Then we require that the following be true of f :

1. $S_0(f)$ is empty.
2. $S_1(f)$ consists of smooth non-intersecting curves. We call these the *fold curves* of f .
3. The set of points where $f|_{S_1(f)}$ has zero differential is empty.
4. If $p \in S_1(f)$ then there exist coordinates (u, z_1, z_2) centred at p and (x, y) centred at $f(p)$ such that f takes the form of either

$$(a) \ (x, y) = (u, \pm(z_1^2 + z_2^2)), \text{ or}$$

$$(b) \ (x, y) = (u, \pm(z_1^2 - z_2^2))$$

in a neighbourhood of p . If f takes the form of 4a then we further classify p as a *definite fold*, and if f takes the form of 4b then p is an *indefinite fold*.

5. Let $\gamma_i, \gamma_j, \gamma_k \in S_1(f)$ be fold curves. Then $f(\gamma_{i,j,k})$ are submanifolds of \mathbb{R}^2 such that
 - (a) $f(\gamma_i)$ and $f(\gamma_j)$ intersect transversely,
 - (b) $f(\gamma_i) \cap f(\gamma_j) \cap f(\gamma_k)$ is empty (i.e. there are no triple-intersections), and
 - (c) self-intersections of $f(\gamma_i)$ are transverse
6. The set of singular values of f in the plane is connected
7. The image of M through f is bounded in the plane.

We call these the *stratification conditions* on f , and we call a map satisfying the stratification conditions a *stratifying map*. The existence of smooth maps satisfying conditions 1–4 is discussed in [1], and 5–7 are straightforward. A smooth map satisfying conditions 1–4 can be smoothly perturbed inside of a tubular neighbourhood of $S_1(f)$ to satisfy conditions 5 & 6. Finally, condition 7 is always satisfied because the image of a compact set through a continuous map is compact.

3.2 Stratifying \mathbb{R}^2

Let $f : M \rightarrow \mathbb{R}^2$ be a smooth map possessing the stratification conditions of Section 3.1 and let $X_f = f(S(f))$, the set of singular values of f . X_f is a connected collection of arcs in the plane that intersect only transversely.

We fit closed neighbourhoods (*sleeves*) around the singular values of f and classify these sleeves by the maximum codimension (with respect to \mathbb{R}^2) of singular values they contain. Because X_f consists of codimension 1 and codimension 2 singular values (i.e. arcs and arc-crossings respectively), we stratify \mathbb{R}^2 into face regions that contain no singular values, edge regions that contain only codimension 1 singular values, and vertex regions, each of which contain exactly 1 codimension 2 singular value. Figures 3.1-3.3 are used to illustrate the stratification resulting from sleeve-fitting.

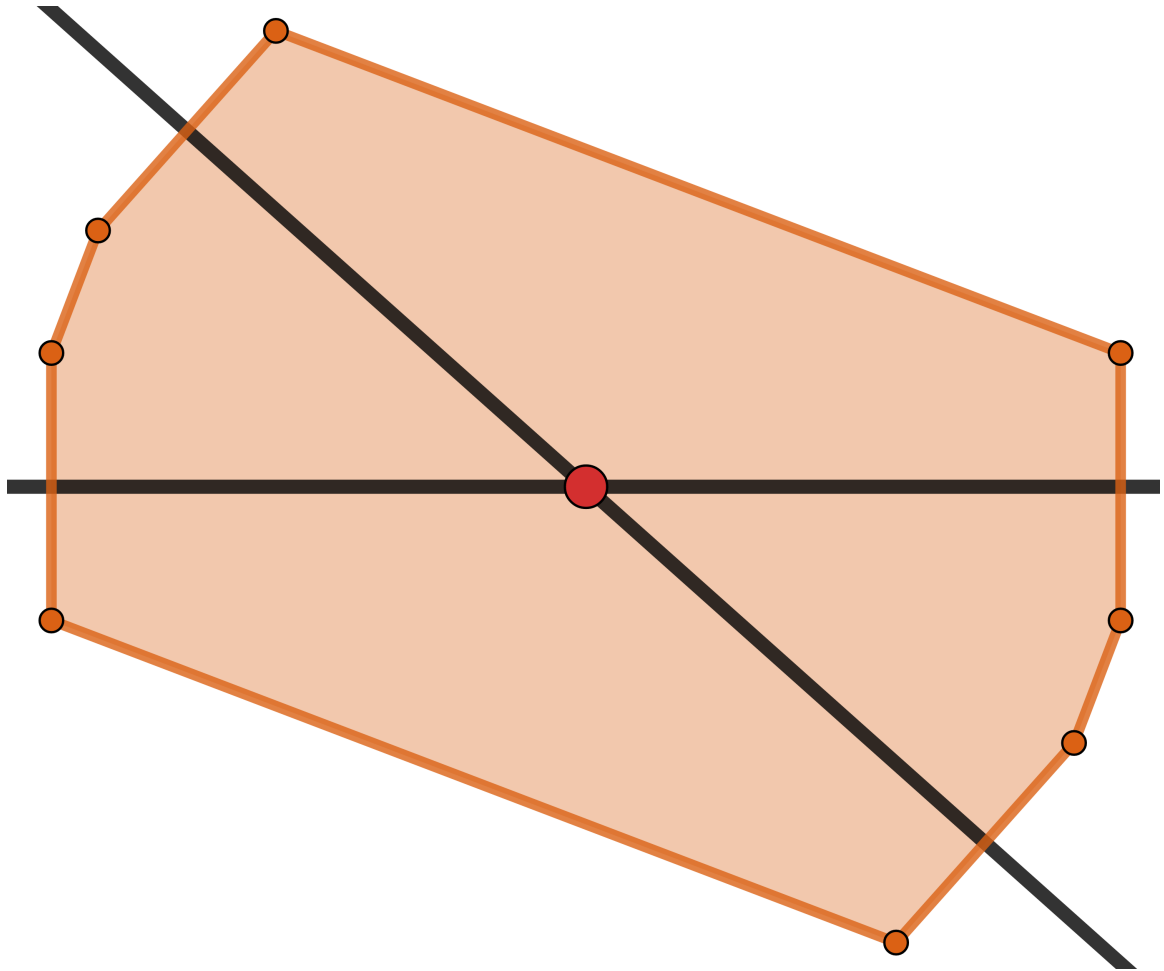


Figure 3.1: **Forming vertex regions.** Octagonal sleeves are fit around codimension 2 singular values to form vertex regions.

We begin by fitting octagonal sleeves around codimension 2 singular values as in Figure 3.1. Let x be a codimension 2 singular value. x is the result of an arc crossing, and a small neighbourhood around an arc crossing is divided into four regions of regular values. The octagon around x is fit so its edges alternate between being fully contained in a region of regular values and orthogonally intersecting one of the arcs of singular values that creates x . See Figure 3.1 for a model fitting.

The interiors of the octagons along with the octagonal boundaries form the vertex regions of the stratification of \mathbb{R}^2 . The octagons are chosen to be small enough that no two vertex regions overlap and such that the octagonal edges that intersect arcs of codimension 1 singular values are all the same length.



Figure 3.2: **Forming edge regions.** Vertex region corners are connected to fit sleeves around arcs of codimension 1 singular values to form edge regions.

Let γ be an arc of codimension 1 singular values with endpoints a pair codimension 2 singular values. γ orthogonally intersects one edge from each of the octagonal vertex regions fit around its endpoints, and we use these edges to form the edge region associated to γ by connecting the endpoints of these edges to one another using a pair of arcs parallel to γ . See Figure 3.2 for a model fitting.

The closures of the interiors of the shapes formed by the arcs and octagon edges form the edge regions of the stratification of \mathbb{R}^2 . The octagonal edge endpoints are also vertices of the octagons, and the formation of edge regions uses every octagonal vertex as the endpoint of exactly one arc.

Removing from $f(M)$ all vertex and edge regions, we are left with a collection of simply connected regions in the plane, each of which consists entirely of regular values. We take the closures of these to be the face regions of the stratification of \mathbb{R}^2 . The boundary of each face region is an alternating collection of arcs from edge regions and octagonal edges from vertex regions. See Figure 3.3 for a model fitting.

With all of the regions defined, we can describe precisely how f stratifies \mathbb{R}^2 . The first collection of subsets used to filter \mathbb{R}^2 are the corners of the octagonal vertex

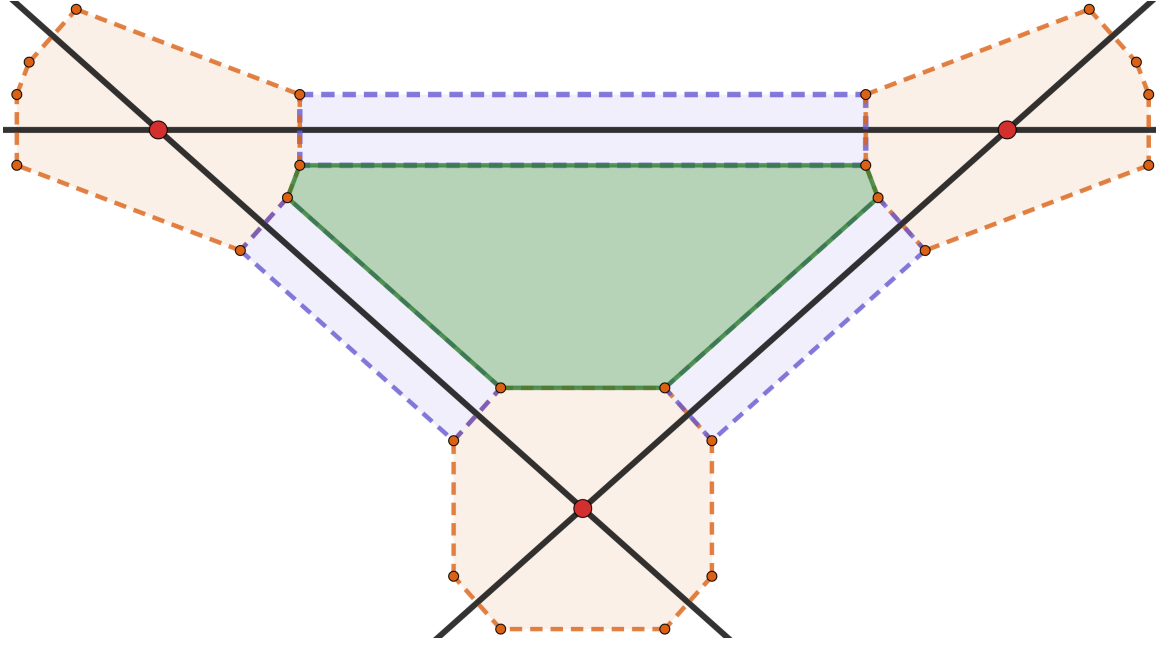


Figure 3.3: **Forming face regions.** All remaining regions contain no singular values, and we take these to be the face regions.

sleeves. We assign to these subsets the indices $(0, i)$ for $i = 1 \dots N_0$, where N_0 is the number of corners. Corners are disjoint, so $(0, i) \not\leq (0, j)$ for any i, j .

The boundary arcs connect the $(0, i)$ -level strata. Arcs are indexed by $(1, j)$ for $j = 1 \dots N_1$, where N_1 is the number of arcs. The boundary points of an arc are corners and are subsets of the filtration indexed by the $(0, i)$ indices, so $(0, i) \leq (1, j)$ if and only if $M_{(0, i)}$ is one of the boundary points of $M_{(1, j)}$. Arcs intersect only at their boundary points, so $(1, j) \not\leq (1, k)$ for any j, k .

The regions themselves are indexed by $(2, k)$ for $k = 1 \dots N_2$, where N_2 is the number of regions. These indices work similarly to the arc indices. The boundary of a region consists of corners and arcs, so $(n, i) \leq (2, k)$ if and only if $M_{(n, i)}$ is contained in the boundary of $M_{(2, k)}$.

3.3 Stratifying M

Stratifying \mathbb{R}^2 via the singular values of f also induces a stratification of M by considering the fibers of f above the stratifying regions. The interiors of face regions have preimage through f a disjoint collection of face blocks, the interiors of edge regions have preimage of edge blocks, and of vertex regions, vertex blocks.

To understand the structure of face, edge, and vertex blocks we investigate the preimages of regular and singular values of f in the plane.

Definition 3.3.1. Because M is closed, f is proper. Thus, for any point q in $f(M)$, a fiber of f above q (i.e. a connected component of $f^{-1}(q)$) is either a closed 1-manifold (i.e. S^1) or contains a critical point of f .

We define a *singular fiber* to be a fiber that contains a critical point of f , and a *regular fiber* to be a fiber consisting entirely of regular points.

The subsets used to stratify M are the fibers of f above the corners of the octagonal vertex regions, the edges of the vertex and edge regions, and the regions themselves. Because the corners of the vertex regions are regular values, their fibers are regular, hence a finite collection of disjointly embedded circles in M . We take these circles as the first collection of subsets that filter M , and assign to them the indices $(1, i)$ for $i = 1 \dots N_1$, where N_1 is the number of circles. These circles are disjoint, so $(1, i) \not\leq (1, j)$ for any i, j .

The arcs of the decomposition connect the vertices and either consist entirely of regular values or contain exactly one singular value. When an arc contains exactly one singular value, exactly one fiber above that value is a singular fiber, with the rest regular fibers. A decomposing arc is diffeomorphic to the unit interval and f is a smooth submersion between smooth manifolds, so a fiber above a decomposing arc is a surface with boundary the fibers above the arc endpoints. When the fiber is regular, the surface is diffeomorphic to an annulus $S^1 \times [0, 1]$. When the fiber is singular, the surface classification depends on the type of singularity. Theorem 3.3.2 and Figure 3.4 show that the fiber containing the singularity either has the structure of a figure-of-eight (when the singularity is part of an indefinite fold) or is a single point (when the singularity is part of a definite fold), hence the singular fiber above the arc is diffeomorphic to either a 2-disk or a pair-of-pants.

Theorem 3.3.2 refers to a *stable map*, and we'll denote the set of smooth stable maps $X \rightarrow Y$ by $Stab(X, Y)$. When X is a smooth, closed, orientable 3-manifold and Y is the plane, $Stab(X, Y)$ consists of all maps $X \rightarrow Y$ satisfying the first five stratification conditions. The last stratification condition is trivially satisfied because X is closed, hence the set of stratifying maps $X \rightarrow Y$ is the subset of $Stab(X, Y)$ consisting of maps f such that $f(S(f))$ is connected.

Theorem 3.3.2 (Adapted Theorem 3.15 in Saeki [3]). Let $f : M \rightarrow N$ be a proper C^∞ stable map of an orientable 3-manifold M into a surface N . Then, every singular

fiber of f is equivalent to the disjoint union of:

1. one of the fibers in Figure 3.4, and
2. the disjoint union of a finite number of copies of S^1 .

Furthermore, no two fibers in the list are equivalent to each other even after taking the union with regular circle components.

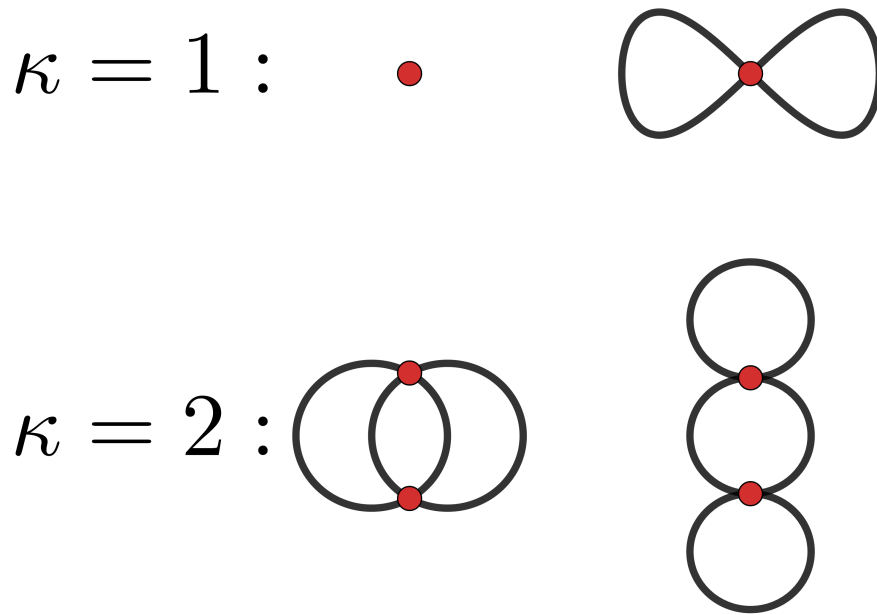


Figure 3.4: **Connected singular fibers.** List of connected singular fibers of proper C^∞ stable maps of orientable 3-manifolds into surfaces. κ is the codimension of the singularity in the surface. The singular fiber above a codimension 2 singular value may be disconnected, in which case the fiber is the disjoint union of a pair of singular fibers from $\kappa = 1$.

The surface fibers above the decomposing arcs are the second collection of subsets that filter M , and they are assigned the indices $(2, j)$ for $j = 1 \dots N_2$, where N_2 is the number of surfaces. The boundary circles of the surfaces are each subsets of the filtration, indexed by the $(1, i)$ indices, so $(1, i) \leq (2, j)$ if and only if $M_{(1, i)}$ is one of the boundary components of $M_{(2, j)}$. These surfaces intersect one another only when they share a boundary circle, so $(2, j) \not\leq (2, k)$ for any j, k .

There are three types of region in the decomposition: face, edge, and vertex. Regardless of the type of region, they are indexed in our filtration similarly to the edges. A fiber above a region is a 3-manifold with corners formed by the $(1, i)$ - and

$(2, j)$ -level strata, and fibers are disjoint away from their boundaries. We therefore index fibers above regions with the indices $(3, k)$ for $k = 1 \dots N_3$ where N_3 is the total number of fibers above regions, put $(n, i) \leq (3, k)$ if and only if $M_{(n, i)}$ is contained in the boundary of $M_{(3, k)}$.

Recall that we call a closed 3-dimensional stratum of M a *block*. We now prove that the stratification conditions impose the desired structure on the blocks of M , as discussed in the introduction to this chapter.

Theorem 3.3.3. Let M be a smooth, closed, orientable 3-manifold, let $f : M \rightarrow \mathbb{R}^2$ be a stratifying map, suppose \mathbb{R}^2 has been decomposed as in Section 3.2 and M has been stratified as in this section. Then each closed strata $M_{(3, k)}$ is classified as either a *face*, *edge*, or *vertex block* depending on whether it is a fiber above a face, edge, or vertex region respectively, and a block has one of the following structures:

- *face block*: Let B be a face block and let F be the face region that B is a fiber over. Then B is homeomorphic to $S^1 \times F$.
- *edge block*: Let B be an edge block and let E be the edge region that B is a fiber over. Let A be the annulus $S^1 \times [0, 1]$ and P the pair-of pants surface (i.e. D^2 minus a pair of disjoint open balls). If B is a regular fiber over E then B is homeomorphic to $S^1 \times E$, hence also homeomorphic to $A \times [0, 1]$. Otherwise, B is a singular fiber over E and contains part of definite or indefinite fold. In this case we call B a *definite* or *indefinite edge block*. A definite edge block is homeomorphic to $D^2 \times [0, 1]$ and an indefinite edge block is homeomorphic to $P \times [0, 1]$.
- *vertex block*: Let B be a vertex block and let V be the vertex region that B is a fiber over. If B is a regular fiber then it is homeomorphic to $S^1 \times V$, therefore homeomorphic to a $(3, 1)$ -handlebody of genus 1. Otherwise, we see from Figure 3.4 that the singular fiber above the codimension 2 singularity contained in V is either connected or disconnected. If the singular fiber is disconnected then there are a pair of disjoint vertex blocks that each contain one of the singular fibers, hence part of a definite or indefinite fold. We therefore classify these blocks as *definite* or *indefinite vertex blocks*. If the singular fiber is connected, then the block containing it is an *interactive vertex block*. A definite(resp. indefinite) vertex block extends and connects definite(resp. indefinite) edge blocks, and is

homeomorphic to a $(3, 1)$ -handlebody of genus 0 (resp. 2). An interactive vertex block is homeomorphic to a $(3, 1)$ -handlebody of genus 3.

Remark 3.3.4. The structures of the blocks described in Theorem 3.3.3 are roughly disk bundles over a representative fiber for the given region. For a block that is a regular fiber, the representative is a circle. For a definite or indefinite block, the representative is the singular fiber containing a definite or indefinite fold, and for an interactive block the representative fiber is the singular fiber above the codimension 2 singular value.

Proof of Theorem 3.3.3. We split the proof into three parts. The first part proves that if a block B is a regular fiber over the region R then B is homeomorphic to $S^1 \times R$. In the second part, we prove that definite and indefinite blocks are homeomorphic to $D^2 \times [0, 1]$ or $P \times [0, 1]$ respectively. In the final part we discuss interactive vertex blocks, and show that they are homeomorphic to $(3, 1)$ -handlebodies of genus 3. Figures illustrate the block structures.

Part 1: Let B be a block over the region R , and suppose B consists entirely of regular fibers over R . Then $(B, R, f|_B, S^1)$ has the structure of a circle bundle over R . A fiber bundle over a contractible space is trivial, so B is homeomorphic to $S^1 \times R$. Furthermore, this homeomorphism is stratified by ensuring the strata of B are mapped to the strata of $S^1 \times R$, where the stratification of $S^1 \times R$ is defined by the manifold with corners structure induced by the product topology. See Figure 3.5.

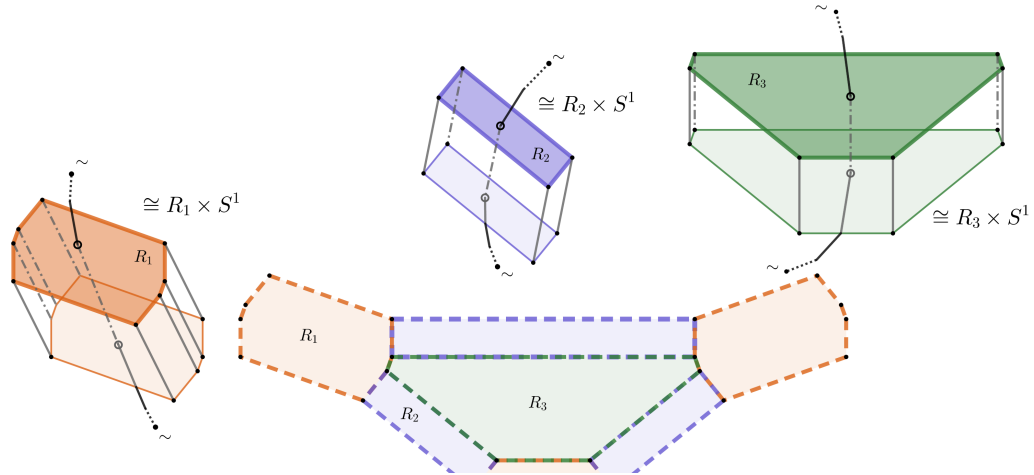


Figure 3.5: **Regular blocks.** Three types of regular blocks. These are found as regular fibers over face, edge, and vertex regions.

Part 2: Let B be a definite or indefinite block over the region R . R is a subset of

the plane homeomorphic to D^2 with an arc $\gamma_s \subset X_f$ of singular values running from one of its edges to another. Let γ_t be a second simple arc that crosses γ_s transversely, and consider the cross-sectional surface obtained by $f^{-1}(\gamma_t)$. Figure 3.6 illustrates the possible surfaces containing the singular fiber over $x = \gamma_s \cap \gamma_t$.

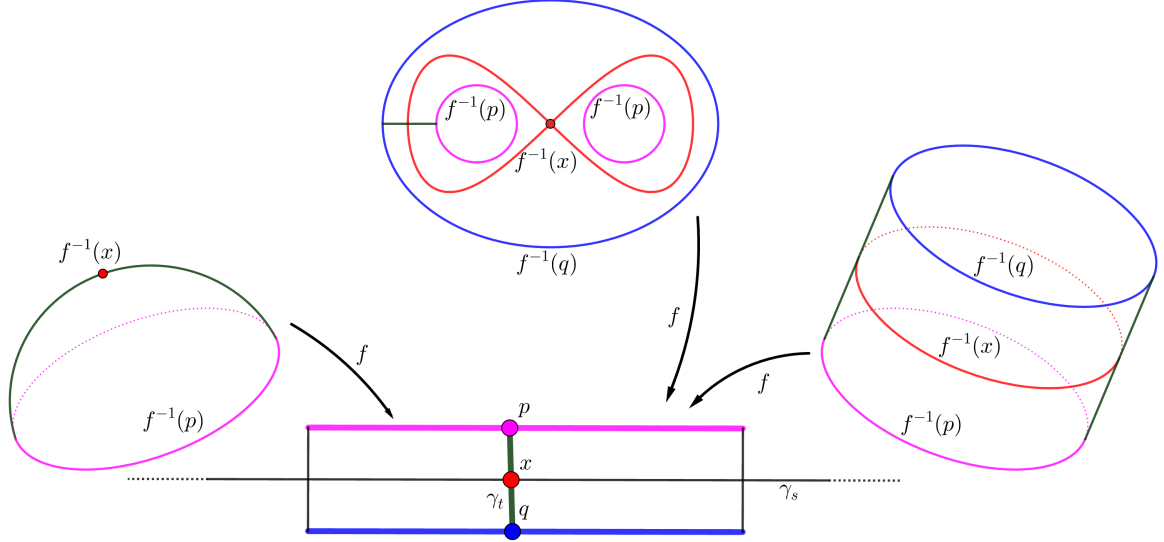


Figure 3.6: **Surfaces over codimension 1 singularities.** γ_s is an arc of singular values and γ_t is an arc with endpoints $\partial\gamma_t = \{p, q\}$ that intersects γ_s transversely at $x = \gamma_s \cap \gamma_t$. The three surfaces shown are the three possible cross-sectional surfaces that can project through f over γ_t .

This cross section is general, so we fit a tubular neighbourhood $\nu(\gamma_s)$ about γ_s in R to obtain a bundle structure for $f^{-1}(\nu(\gamma_s))$ whose fiber is one of the cross-sectional surfaces (a disk or a pair-of-pants) and whose base is the arc γ_s , i.e. an interval. The interval is contractible, so $f^{-1}(\nu(\gamma_s))$ is homeomorphic to $\Sigma \times [0, 1]$ for Σ a disk or a pair-of-pants surface. Away from $\nu(\gamma_s)$, R consists entirely of regular values so we obtain solid tori (cf. Part 1) that extend the $\Sigma \times [0, 1]$ structure as seen in Figure 3.7.

Figure 3.7: **Definite and indefinite blocks.** The blocks containing sections of definite and indefinite folds that project over codimension 1 singular values. These are found as singular fibers over edge and vertex regions.

As with Part 1, the homeomorphism described is stratified by ensuring the strata of B are mapped to the strata of $\Sigma \times [0, 1]$, where the stratification of $\Sigma \times [0, 1]$ is defined by the manifold with corners structure induced by the product topology.

Part 3: Let B be an interactive block over the region R . Interactive blocks occur over octagonal vertex regions where the singular fiber above the region's codimension 2 singularity is connected, so we investigate these fibers. The codimension 2 singular value lies at the intersection of a pair of arcs of codimension 1 singular values. Call the arcs γ_1 and γ_2 , let $x = \gamma_1 \cap \gamma_2$, and denote the interactive singular fiber over x by $B_x = B \cap f^{-1}(x) = \{b \in B \mid f(b) = x\}$. Our method of investigation begins by examining the possible resolutions of B_x and combining those resolutions to form a genus 3 surface.

Figure 3.8 demonstrates resolutions of the singular points of B_x when B_x has the first interactive singular fiber form presented in Figure 3.4. We first note that all of the displayed fibers have inherited an orientation from M . This forces fiber resolution to be unambiguous, and allows us to identify fibers when forming the surface shown in Figure 3.9.

Figure 3.8: **Resolutions of the singular points in the first interactive fiber.** B_x and its possible resolutions over nearby codimension 1 singular values and regular values. The fibers inherit orientation from M , and this illustration is presented without loss of generality.

We form the surface shown in Figure 3.9 by gluing together the surfaces that project over simple arcs transversing over the codimension 1 singular values. Gluing is performed over the boundary circles of these surfaces, and is prescribed by the resolutions in Figure 3.8. In the first case, we obtain four pair-of-pants surfaces and two cylinders, and these glue together to form a genus 3 surface.

Figure 3.9: **Surface Σ near the first interactive fiber that projects over $\partial\nu(x)$.** The surface and B_x are presented as embedded in S^3 , where $H(B_x)$ is the genus-3 (3,1)–handlebody on the ‘outside’ of Σ in S^3 .

The surface Σ in Figure 3.9 is the boundary of $H(B_x)$, a regular neighbourhood of B_x in M , i.e. a genus-3 (3,1)–handlebody inside of M . $H(B_x)$ projects through f over $\bar{\nu}(x)$, a closed tubular neighbourhood of x , and Σ projects over $\partial(\nu(x))$.

Figure 3.9 presents Σ and B_x as objects embedded in S^3 , where Σ bounds genus-3 (3,1)–handlebodies on both sides. We take the ‘outside’ component of $S^3 \setminus \Sigma$ (i.e. the component containing B_x) to be our model $H(B_x)$.

Outside of $\nu(x)$ we use the investigations from Parts 1 and 2 of this proof. The rest of R , $f^{-1}(R \setminus \nu(x))$, has the structure of a Σ -bundle over the interval, and the bundle

extends $H(B_x)$ to the boundary of R , preserving the structure as a genus-3 (3,1)–handlebody. We conclude that B is homeomorphic to a genus-3 (3,1)–handlebody.

An identical argument is made when B_x has the second interactive singular fiber form, using Figures 3.10 and 3.11 in place of Figures 3.8 and 3.9 respectively.

Figure 3.10: Resolutions of the singular points in the second interactive fiber. B_x and its possible resolutions over nearby codimension 1 singular values and regular values. The fibers inherit orientation from M , and this illustration is presented without loss of generality.

Figure 3.11: Surface Σ near the second interactive fiber that projects over $\partial\nu(x)$. The surface and B_x are presented as embedded in S^3 , where $H(B_x)$ is the genus-3 (3,1)–handlebody on the ‘outside’ of Σ in S^3 .

Figure 3.12 displays both possible interactive block structures, highlighting their boundaries. The figure explains that the blocks are the handlebodies on the ‘outside’ of the illustrated surfaces. This is specifically to aid visualization of the effects of 2– and 3–handle attachment in the next two sections, as the result of these attachments will fill the genus-3 (3,1)–handlebody on the ‘inside’ of the illustrated surface.

Figure 3.12: Possible interactive block structures embedded in S^3 . Interactive blocks with indicated boundary stratification induced by $f^{-1}\partial R$. Blocks are embedded in S^3 , outside of the illustrated stratified boundary surfaces.

□

A smooth map f satisfying the stratification conditions of Section 3.1 induces a decomposition on \mathbb{R}^2 and a stratification of M . It is important to note here that the restrictions on f can induce a wide variety of possible stratifications of M , highlighting the variability of the resulting 4–manifold. We end this section with a lemma that guarantees the stratified 2–handle attachments of the next section can be made over our face blocks in any order, hence we can assume all attachments occur simultaneously.

Lemma 3.3.5. Let M be a 3–manifold with stratification induced as in Theorem 3.3.3. Then blocks of the same type (i.e. face, edge, vertex) are disjoint.

Proof. The fibers of the blocks are disjoint, so blocks of the same type may only intersect on their boundary. A block's boundary is induced by the boundary of the region it projects over and regions of the same type intersect nowhere, hence their corresponding blocks intersect nowhere. \square

3.4 Attach Handles

Stratifying M allows the definition of attachment neighbourhoods for stratified 2-, 3-, and 4-handles in $W = M \times [0, 1]$. A 4-dimensional 2-handle is attached over a closed solid torus embedded in the boundary of a 4-manifold, so attachment neighbourhoods for our stratified 2-handles are straightforward: they are the face blocks of M . We alter the boundary of W by attaching handles, so the attachment neighbourhoods for 3-handles (4-handles, resp.) must be found after 2-handles (3-handles, resp.) are attached. For 3-handles, an attachment neighbourhood consists of the union of an edge block with some strata introduced by 2-handle attachment. For 4-handles, an attachment neighbourhood consists of the union of an edge block with some strata introduced by 2- and 3-handle attachment. We investigate the consequences of handle attachment by comparing the boundary of the initial manifold with the boundary of the manifold resulting from handle attachment, and use a precisely defined handle structure to focus the investigation. Our first step is to precisely define the structure of the stratified 2-handles that we are attaching.

3.4.1 2-handles

Let B be a face block of M_1 . By Theorem 3.3.3, B is a closed solid torus that is stratified-homeomorphic to $S^1 \times G_n$, where G_n is an n -gon for some n . Consider an unknotted embedding of B in S^3 , as illustrated in Figure 3.13. The complement of the interior of B is another closed solid torus B' , and we stratify B' as follows. First include the shared stratified boundary of B . Next, introduce meridinal disks of B' that are bounded by the $(1, i)$ -indexed strata in B , i.e. the boundary curves in B corresponding to $S^1 \times c_m$ where c_m is a corner of G_n , $m = 1 \dots n$. Finally, add the homeomorphic 3-disks of B' whose boundaries consist of one longitudinal annulus of B along with the two meridinal disks in B' that are bounded by the annulus's circular boundary components. The filtration of B' is created identically to that of the original face blocks, using inclusion as a partial ordering and indexing a stratum

by its dimension as a submanifold of B' . Figure 3.13 illustrates a face block B and its complement inside of S^3 .

Figure 3.13: A face block and its complement inside of S^3 . A face block B is a stratified closed solid torus that is stratified-homeomorphic to $S^1 \times G_n$ for some n -gon G_n . The complement of its unknotted interior in S^3 is another stratified closed solid torus B' .

Taking S_B^3 to be the stratified S^3 formed as the union of B and B' , we craft a stratified 2-handle structure as $C(S_B^3)$, the cone of S_B^3 . We call $C(S_B^3)$ the *stratified 2-handle induced by B* . Attaching $C(S_B^3)$ to W over $B \subset M_1$ alters the boundary of W by replacing $B \subset M_1$ with B' . The full extent of this surgery can be detected by examining the edge and vertex blocks of the stratification that are incident to B .

Theorem 3.4.1. Let M be a smooth, closed, stratified, orientable 3-manifold with stratification induced by a stratifying map f , let \mathfrak{B} be the set of face blocks of M_1 , and let $W = M \times [0, 1]$. Consider the 4-manifold W' constructed from W as

$$W' = W \cup \{C(S_B^3)\}_{B \in \mathfrak{B}} / \sim,$$

where \sim is defined by $b \sim \iota(b)$, ι the identity map $C(S_B^3) \supset B \xrightarrow{\iota} B \subset M_1$. Then $M'_1 = \partial W' \setminus M_0$ is a stratified 3-manifold with a decomposition into *primed edge blocks* and *primed vertex blocks* such that the decomposition is well-defined and the primed blocks have the following structure:

- *primed edge block:* Let E' be a primed edge block. Then E' is identical to an edge block E from Theorem 3.3.3 with cylinders (copies of $D^2 \times [0, 1]$) glued over all annular boundary strata of E (i.e. each closed strata A of E such that $A = E \cap B$ for some face block $B \in \mathfrak{B}$). Thus E' is a stratified 3-manifold homeomorphic to $S^2 \times [0, 1]$
- *primed vertex block:* Let V be a primed vertex block. Then V is identical to a vertex block from Theorem 3.3.3 with cylinders glued over each annular boundary stratum A of V such that $A = V \cap B$ for some face block $B \in \mathfrak{B}$. Thus V is a stratified 3-manifold whose boundary components are each homeomorphic to S^2 .

Proof. We split the proof of this theorem into three parts. In the first two parts, we

prove that we can find the prescribed primed edge and vertex block structures in M'_1 . In the third part, we show that these structures exhaust M'_1 .

Part 1: Edge blocks occur in three possible forms: regular edge blocks as $A \times [0, 1]$, definite edge blocks as $D^2 \times [0, 1]$, and indefinite edge blocks as $P \times [0, 1]$. Figure 3.14 displays the possible edge block forms and indicates the boundary strata of an edge block that are shared by face blocks.

Figure 3.14: **Edge blocks.** The possible edge blocks of M_1 . Annular boundary strata that are incident with face blocks of M_1 have been indicated. Gluing cylinders over the indicated annuli results in a stratified 3-manifold homeomorphic to $S^2 \times [0, 1]$.

Figure 3.15 shows the annulus shared by a model edge block E and B in M_1 and its corresponding annulus shared by B and B' in S^3_B . The figure demonstrates that the effect on ∂W near E of attaching $C(S^3_B)$ over B is equivalent to gluing a well-defined cylinder from the stratification of B' to E over the annular boundary stratum $E \cap B$. Attachment of all 2-handles applies this cylinder gluing to all annular strata of E , and applying this cylinder gluing to all annular strata of E results in a 3-manifold homeomorphic to $S^2 \times [0, 1]$.

Figure 3.15: **The effect of stratified 2-handle attachment on a model edge block.** A model edge block E , a face block B , its complement B' , and the effect of attaching $C(S^3_B)$ to W over B on E . The boundary stratum shared by E and B in M_1 is indicated, as is the corresponding boundary stratum of B' in S^3_B .

Part 2: Vertex blocks occur in five possible forms: regular vertex blocks as S^1 -bundles over the vertex region, indefinite and definite vertex blocks stratified-homeomorphic to those that appear in Figure 3.7, and interactive vertex blocks stratified-homeomorphic to those that appear in Figure 3.12. Figure 3.16 displays the possible vertex block forms embedded in S^3 and indicates the boundary strata of a vertex block that are shared by face blocks.

Figure 3.16: **Vertex blocks.** The possible vertex blocks of M_1 . Annular boundary strata that are incident with face blocks of M_1 have been indicated. Gluing cylinders over the indicated annuli results in a stratified 3-manifold whose boundary is a collection of stratified 2-spheres.

Figure 3.17 displays a model vertex block V embedded on the ‘outside’ of its stratified genus-3 boundary surface in S^3 , and shows the annulus shared by V and

B in M_1 and its corresponding annulus shared by B and B' in S_B^3 . The figure demonstrates that the effect on ∂W near V of attaching $C(S_B^3)$ over B is equivalent to gluing a well-defined cylinder from the stratification of B' to V over the annular boundary stratum $V \cap B$. Attachment of all 2–handles applies this cylinder gluing to all annular strata of V shared by face blocks, and applying this cylinder gluing to such annular strata of V results in a 3–manifold whose boundary components are each homeomorphic to S^2 . Moreover, these boundary components are exactly the boundary components of the primed edge blocks.

Figure 3.17: The effect of stratified 2–handle attachment on a model vertex block. A model edge block V , a face block B , its complement B' , and the effect of attaching $C(S_B^3)$ to W over B on V . The boundary stratum shared by V and B in M_1 is indicated, as is the corresponding boundary stratum of B' in S_B^3 .

Part 3: To show that primed edge and vertex blocks exhaust M'_1 , we show that the entirety of B' has been apportioned among the primed blocks for each B' . The $(3, k)$ strata of B' are each cylinders whose annular boundary strata corresponds directly to a longitudinal boundary annulus of B . Such an annulus projects through f to a boundary edge of a face region. Face regions do not intersect even on their boundary, so all of the annular boundary strata of B , hence B' , are shared only by edge and vertex blocks. Thus each cylinder of B' has been assigned to a primed edge or vertex block. Because 2–handle attachment altered M_1 to M'_1 only by replacing each face block B with its complementary B' , the primed blocks must exhaust M'_1 . \square

Decomposing M'_1 into primed edge and vertex blocks provides us with stratified 3–handle attachment neighbourhoods. A 4–dimensional 3–handle is attached over an $S^2 \times [0, 1]$ embedded in the boundary of a 4–manifold, so attachment neighbourhoods for our stratified 3–handles are the primed edge blocks of M'_1 . We begin 3–handle attachment by precisely defining the structure of a stratified 3–handle so that it may be attached over a primed edge block.

3.4.2 3–handles

Let E' be a primed edge block of M'_1 . By Theorem 3.4.1, E' is homeomorphic to $S^2 \times [0, 1]$. In particular, $\partial E'$ is a disjoint pair of stratified 2–spheres. We form a 4–disk containing E' in its boundary by a double coning method on E' : we first cone

the spherical boundary components of E' to form a 3-disk, then cone the 3-disk to obtain a 4-disk.

For each stratified boundary sphere $S_i^2 \in \partial E'$ we form the stratified 3-disk $C(S_i^2)$ and glue $C(S_i^2)$ to E' over S_i^2 . The result is a stratified 3-disk, and we further cone that 3-disk to form a stratified 4-disk. We denote the 4-disk by $C^2(E')$ and call the resulting stratified 3-handle structure the *stratified 3-handle induced by E'* . Attaching $C^2(E')$ to W' over $E' \subset M'_1$ alters the boundary of W' by replacing E' with the 3-disks $C(S_i^2)$ glued over the corresponding stratified boundary spheres in M'_1 . The full extent of this surgery can be detected by examining the primed vertex blocks of M'_1 .

Corollary 3.4.2. Let W' be the 4-manifold resulting from the construction described in Theorem 3.4.1 and let \mathfrak{E}' be the set of primed edge blocks of $M'_1 \subset \partial W'$. Consider the 4-manifold W'' constructed from W' as

$$W'' = W' \cup \{C^2(E')\}_{E' \in \mathfrak{E}'} / \sim,$$

where \sim is defined by $e \sim \iota(e)$, ι the identity map $C^2(E') \supset E' \xrightarrow{\iota} E' \subset M'_1$. Then $M''_1 = \partial W'' \setminus M_0$ is a stratified 3-manifold with a decomposition into *double primed vertex blocks* V'' such that the decomposition is well-defined and each V'' is homeomorphic to S^3 .

Proof. For each vertex block V , the cylinders introduced by 2-handle attachment and the 3-disks introduced by 3-handle attachment combine into a handlebody H of the same genus as V . V and H combine to form each component of M''_1 , and we show a Heegaard diagram of complementary meridional circles for each case in Figures 3.18-3.22. Thus M''_1 consists of a collection of stratified 3-spheres [4].

Figure 3.18: Heegaard system for genus-0 vertex blocks. V is a genus-0 handlebody when V is a definite singular fiber of f . There is only one possible Heegaard diagram for genus-0 handlebodies, and the result is trivially S^3 .

Figure 3.19: Heegaard system for genus-1 vertex blocks. V is a genus-1 handlebody when V is a regular fiber of f . The Heegaard diagram consists of a meridian of each of V and H .

□

Figure 3.20: **Heegaard system for genus-2 vertex blocks.** V is a genus-2 handlebody when V is an indefinite singular fiber of f . The Heegaard diagram for H consists of the pants cuffs, and for V the side seam.

Figure 3.21: **Heegaard system for genus-3 vertex blocks, case 1.** V is a genus-3 handlebody when V contains an interactive singular fiber. There are two types of interactive singular fibers, we show here the first from Figure 3.4

Figure 3.22: **Heegaard system for genus-3 vertex blocks, case 2.** V is a genus-3 handlebody when V contains an interactive singular fiber. There are two types of interactive singular fibers, we show here the second from Figure 3.4

After attaching 3–handles over primed edge blocks, W'' is a 4–manifold with boundary consisting of M_0 and a collection of stratified 3–spheres. We attach stratified 4–handles over these 3–spheres, so we begin by precisely defining the structure of these handles.

3.4.3 4–handles

Let V'' be a double primed vertex block of M_1'' . By Theorem 3.4.2, V'' is homeomorphic to S^3 . We form a 4–disk whose boundary is V'' by taking the cone of V'' . We denote this 4–disk by $C(V'')$ and call the resulting 4–handle structure the *stratified 4–handle induced by V''* . Attaching $C(V'')$ to W'' over V'' alters the boundary of V'' by replacing it with \emptyset .

Corollary 3.4.3. Let W'' be the 4–manifold resulting from the construction described in Theorem 3.4.2 and let \mathfrak{V}'' be the set of double primed vertex blocks of $M_1'' \subset \partial W''$. Consider the 4–manifold W''' constructed from W'' as

$$W''' = W'' \cup \{C(V'')\}_{V'' \in \mathfrak{V}''} / \sim,$$

where \sim is defined by $v \sim \iota(v)$, ι the identity map $C(V'') \supset V'' \xrightarrow{\iota} V'' \subset M_1''$. Then $M_1''' = \partial W''' \setminus M_0 = \emptyset$, hence W''' is a 4–manifold whose boundary is exactly M .

Chapter 4

Algorithm for constructing a triangulated 4-manifold with prescribed 3-manifold boundary

The steps to construct a triangulated 4-manifold with prescribed closed, orientable 3-manifold boundary broadly follow the steps to construct a 4-manifold with prescribed smooth, orientable 3-manifold boundary. Let N be a closed, orientable 3-manifold triangulation. Then the steps of construction are:

1. Define a projection $f : N \rightarrow \mathbb{R}^2$.
2. Induce a subdivision of N from f . The result is a 3-dimensional cell complex M that is equivalent to N .
3. $M \times [0, 1]$ is a 4-dimensional cell complex with boundary components $M_0 = M \times \{0\}$ and $M_1 = M \times \{1\}$. Let W be the triangulation obtained by inductively triangulating each cell of M .
4. Attach 4-dimensional 2-handles to W over its M_1 boundary as prescribed by the subdivision of M from f . Call the result W' and let $M'_1 = \partial W' \setminus M_0$.
5. Form W'' by attaching 4-dimensional 3-handles to W' over M'_1 as prescribed by the subdivision induced by f and the surgery induced by 2-handle attachment.
6. The boundary of W'' consists of M_0 and a collection of copies of S^3 . Coning the 3-spheres results in a triangulated 4-manifold whose boundary is exactly M_0 .

Each of these steps is made algorithmic, and these algorithms are chained in series to form a single algorithm. This algorithm has input a closed, orientable 3-manifold triangulation N and output a 4-manifold triangulation W''' whose sole boundary component is a triangulated 3-manifold that is equivalent to N in the sense of triangulations. In this case, we find that $\partial W'''$ is a subdivision of N , and this subdivision is the subdivision induced by the projection f in Step 1.

It is necessary that the input 3-manifold triangulation is *edge-distinct*, i.e. if u, v are vertices of N then $\{u, v\}$ is the boundary of at most one edge. If this condition is not satisfied by a given N , then it is satisfied by the barycentric subdivision of N . We assume that N is edge-distinct for the remainder of the chapter.

Throughout this chapter N refers to the input closed, orientable 3-manifold triangulation, f refers to the subdividing map defined in Section 4.1, M is the subdivision of N induced by f , W is the 4-manifold triangulation obtained from $M \times [0, 1]$, W' is the result of attaching 2-handles to W , and W'' is the result of attaching 3-handles to W' .

4.1 Define projection

The projection's utility is in defining a subdivision of the initial closed, orientable 3-manifold triangulation N such that attaching regions for triangulated 2- and 3-handles can be found. This is done before forming the base 4-manifold so that the boundary components of W contain the desired handle attachment sites.

Our subdivision is obtained by imposing four conditions on $f : N \rightarrow \mathbb{R}^2$:

1. f maps vertices to the circle, i.e. for each vertex $v \in N^0$, $f(v)$ lies on the unit circle in \mathbb{R}^2 .
2. The images of vertices are distinct, i.e. for every pair of vertices $u, v \in N^0$, $f(u) \neq f(v)$.
3. f is linear on each simplex of N and piecewise-linear on N , i.e. if $x \in \sigma$ is a point in the simplex σ with vertices v_i , then $x = \sum_i a_i v_i$ with $\sum_i a_i = 1$ and $f(x) = \sum_i a_i f(v_i)$.
4. Edge intersections are distinct, i.e. for every triple of edges $e_1, e_2, e_3 \in N^1$ that share no vertices, $f(e_1) \cap f(e_2) \neq f(e_2) \cap f(e_3)$.

We call these the *subdivision conditions* on f , and we call a map satisfying the subdivision conditions a *subdividing map*. Conditions 1 and 2 ensure that every simplex of N is mapped to the plane in standard position, where a simplex σ of N is mapped to the plane in *standard position* if every point in $f(\sigma^0)$ is essential in forming the convex hull of $f(\sigma^0)$. See Figure 4.1 for an illustration. This, along with conditions 3 and 4, allows us to use concepts and language from normal surface theory to describe the subdivision of N in the next section.

All conditions are satisfied by fixing an odd integer k greater than or equal to the number of vertices in N , injecting the vertices of N to the k^{th} complex roots of unity in the plane, then extending linearly over the skeletons of N . The first three conditions are clearly satisfied by this procedure, and the last is satisfied by the results in [2].

Algorithm 1 takes as input the closed, orientable 3-manifold triangulation N and produces a subdividing map $f : N \rightarrow \mathbb{R}^2$. The subdividing map projects each tetrahedron to the plane in *standard position*, as shown in Figure 4.1.

	Data: A closed, orientable 3-manifold triangulation N
	Result: A subdividing map $f : N \rightarrow \mathbb{R}^2$
1	begin
2	$k =$ the smallest odd number greater than or equal to $ N^0 $
3	foreach vertex v_i in N^0 , $i = 1, \dots, N^0 $ do
4	$f(v_i) = (\cos(\frac{2\pi i}{k}), \sin(\frac{2\pi i}{k}))$
5	end
6	foreach n in $\{1, 2, 3\}$ do
7	foreach simplex σ in N^n do
8	by definition, σ is the set of convex combinations of σ^0 :
9	$\sigma^0 = \{v_0, \dots, v_n\}$
10	$\sigma = \{x \mid x = \sum_{j=0}^n t_j v_j, \sum t_j = 1, t_j \geq 0 \text{ for each } j\}$
11	define f on $x \in \sigma$ by requiring linearity over simplices:
12	$f(x) = f(\sum_{j=0}^n t_j v_j) = \sum_{j=0}^n t_j f(v_j)$
13	end
14	end
15	end

Algorithm 1: Constructing a subdividing map $f : N \rightarrow \mathbb{R}^2$

Figure 4.1: **A tetrahedron σ projected to the plane in standard position through a subdividing map f .** The four vertices of σ^0 map to the unit circle in the plane, thus form a convex arrangement. Four of the six edge of σ^1 map to the boundary of $f(\sigma)$, connecting $f(\sigma^0)$. The last two edges map across $f(\sigma)$, forming an intersection interior to $f(\sigma)$.

4.2 Induce subdivision

The goal of subdividing N is to create and identify handle attachment sites analogous to the face, edge, and vertex blocks of Chapter 3. We use a similar technique to that found in Chapter 3, iteratively subdividing the tetrahedra of N by certain preimages of f . Tetrahedron subdivisions are compatible, i.e. tetrahedron subdivisions fit together exactly as the undivided tetrahedra do inside of N .

Let σ be a tetrahedron of N and let s be a line segment in the plane such that $s \cap f(\sigma)$ is nonempty, the endpoints of s are outside of $f(\sigma)$, and $s \cap f(\sigma)$ is a line segment in $f(\sigma)$ disjoint from any vertices or crossings of $f(\sigma)$. Figure 4.2 demonstrates the possible configurations of these line segments, and shows that their preimages inside of σ are triangles and quads. We refer to these preimages as *exterior triangles* and *exterior quads*. When a pair of these preimages intersect, the intersection is a line segment with endpoints interior to a pair of triangles of σ^2 .

Figure 4.2: **A tetrahedron σ in standard position, intersecting edges, and preimage triangles and quads.** An intersecting edge separates the vertices of σ . If one is separated from the other three, its preimage is a triangle. If the vertices are separated into two pairs of two, the preimage is a quad.

For each $\sigma \in N^3$ and each edge e of N^1 such that $e \notin \sigma^1$, $f(e)$ is a line segment in the plane that is either disjoint from $f(\sigma)$ or induces an exterior triangle or quad in σ . There are two edge of σ whose preimages in σ form *interior triangles*. These are the preimages of the edges of σ that map through f across $f(\sigma)$ as in Figure 4.1, and we refer to these edges as *interior edges*. The three edges of the interior triangle induced by e are e itself along with a pair of edges that bisect the triangles of σ not containing e as an edge. The three vertices of the interior triangle induced by e are the two vertices of σ that are the endpoints of e along with a third vertex located in the edge of σ opposite e . Figure 4.3a shows one interior triangle along with its possible intersections with exterior triangles and quads. The interior triangles of σ

always intersect in a line segment with endpoints inside of the interior edges of σ , shown in Figure 4.3b

- (a) One interior triangle is shown, along with its intersection with an exterior triangle and an exterior quad. (b) Both interior triangles are shown, along with their intersection.

Figure 4.3: **A tetrahedron σ in standard position, interior triangles, and intersections with external triangles and quads.** There are two special preimage triangles in σ , called *interior triangles*, that occur as the preimages of the edges of σ that map through f across $f(\sigma)$ as in Figure 4.1.

Recall that the goal of this subdivision is to identify analogues for the face, edge, and vertex blocks of Chapter 3. If we were to subdivide N using the quads and triangles induced by the edges of N , such analogue blocks are ill-defined. We amend this by introducing a set of line segments that serve the same purpose as the sleeves of Section 3.2.

For each edge e of N^1 , consider $e_\varepsilon^+ = e + \varepsilon_e e_\perp$ and $e_\varepsilon^- = e - \varepsilon_e e_\perp$, line segments in the plane that are parallel to $f(e)$ and located a small orthogonal distance away from $f(e)$. We demand that, for each $e \in N^1$, ε_e is small enough that the rectangle R_e in the plane defined by e_ε^+ and e_ε^- does not fully contain g_ε^\pm for any $g \in N^1$. This requirement also ensures that the only crossings of $f(N^1)$ contained in R_e are crossings involving e . The segments e_ε^\pm for each $e \in N^1$ are called *sleeve segments*, and their preimages form exterior triangles and quads inside of the tetrahedra of N . See Figure 4.4 for an illustration of a pair of sleeve segments.

Figure 4.4: **A pair of sleeve segments in the plane.** We show a pair of edges projections $f(e)$ and $f(g)$ in the plane, along with their associated sleeve segments. Sleeve segments are necessary to ensure well-defined face, edge, and vertex block analogues in the subdivision of N .

Take S to be the set of line segments in the plane that consists of $f(e)$ for each $e \in N^1$ along with the sleeve segments e_ε^\pm . For each tetrahedron σ of N , the triangles, quads, and intersections of $f^{-1}S \cap \sigma$ define a subdivision of σ into a cell complex. Iteration of this subdivision in Algorithm 2 across all tetrahedra of N yields a 3-dimensional cell complex M .

We subdivided N into M in order to identify analogues to the face, edge, and vertex blocks of Chapter 3. The analogous blocks are defined exactly as they were in

<p>Data: A closed, orientable 3-manifold triangulation N with subdividing map $f : N \rightarrow \mathbb{R}^2$</p> <p>Result: A closed, orientable 3-dimensional cell complex M</p> <pre> 1 begin 2 $S = \{f(e) \mid e \in N^1\} \cup \{e_\varepsilon^\pm \mid e \in N^1\}$ 3 foreach tetrahedron σ of N^3 do 4 foreach segment s of S do 5 $\delta =$ the intersection of σ with $f^{-1}s$ 6 replace σ with the 3-dimensional cell complex obtained as σ subdivided by δ 7 end 8 end 9 end </pre>
--

Algorithm 2: Subdividing N

Chapter 3 — the sleeve segments subdivide the plane into regions homeomorphic to disks, those disks are classified by whether they contain a crossing of $f(N^1)$, intersect $f(N^1)$ but do not contain a crossing, or do not intersect $f(N^1)$ at all. The preimage of a region that contains a crossing is a *vertex block analogue*, the preimage of a region that intersects $f(N^1)$ but does not contain a crossing is an *edge block analogue*, and the preimage of a region that is disjoint from $f(N^1)$ is a *face block analogue*. Figure 4.5 illustrates the regions in the plane that produce such blocks. These preimages exhaust the cells of M , providing a decomposition into subcomplexes.

Figure 4.5: **Regions in the plane that correspond to vertex, edge, and face block analogues.** The sleeve segments provide the same functionality as the sleeves in Chapter 3, in that the preimages of the regions they form behave similarly to the vertex, edge, and face blocks defined in Chapter 3.

The Cartesian product of a pair of cell complexes is again a cell complex, so we form the base 4-dimensional cell-complex to which we attach handles as $M \times [0, 1]$. Every cell of $M \times [0, 1]$ is homeomorphic to a disk, so we form a 4-manifold triangulation W as a subdivision of $M \times [0, 1]$. This triangulation is obtained by inductively subdividing each cell of $M \times [0, 1]$ that is not a simplex.

4.3 Attach Handles

At this point in the chapter we have constructed a 4-manifold triangulation W with two boundary components, each equivalent to the 3-dimensional cell complex M obtained in Section 4.2. Furthermore, the cells of M are partitioned into subcomplexes analogous to the face, edge, and vertex blocks of Chapter 3. Explicit attachment sites are available for 2-handles, so our first step is construction of a 2-handle.

4.3.1 Attach 2-handles

The algorithm of this subsection takes as input a pair (T, Γ) where T is a closed solid torus triangulation and Γ is a collection of triangulated disjoint parallel longitudes in the boundary of T . The output is a 4-disk triangulation H satisfying the following:

1. ∂H is a triangulated S^3 with a genus 1 Heegard splitting over ∂T , i.e. $\partial H \setminus \text{int}(T)$ is a solid torus.
2. For each γ_i in Γ , γ_i bounds a triangulated disk in ∂H , i.e. each γ_i is an explicit 0-framing for the 2-handle attachment.

We take H to be a 4-dimensional 2-handle and attach H to W over T . Constructing the 2-handle involves building a solid torus T' that complements T , combining T and T' over their shared boundary to build a triangulated 3-sphere, then coning that 3-sphere into the 4-disk H .

We find pairs (T, Γ) inside of $M_1 \subset \partial W$, the subdivision of N induced by the subdividing map $f : N \rightarrow \mathbb{R}^2$. Let B be a face block analogue of M_1 . B is a 3-dimensional subcomplex of M_1 that forms a closed solid torus, and B projects through f over an n -gon for some n . Call the n corners of $f(B)$ by c_i , $i = 1 \dots n$, and take $C = \{c_1 \dots c_n\}$. Then the $f^{-1}c_i$ are disjoint parallel triangulated longitudes of B . We take $(B, f^{-1}C)$ as our pair (T, Γ) for each face block analogue B of M .

For a closed solid torus T , we find a complementary torus T' , i.e. $\partial T = \partial T'$ as triangulations. We begin by investigating the boundary of T , setting $T'_0 = \partial T$. Inside of T'_0 is the set of disjoint parallel longitudes Γ that are required to bound disks inside of T' , so for each γ_i we attach a disk D_i with $\partial D_i = \gamma_i$ to T'_0 over γ_i . Call the result of these attachments T'_1 . Adjacent longitudes γ_i and γ_j bound an annulus A_{ij} in T'_1 , and $D_i \cup A_{ij} \cup D_j$ is a triangulated 2-sphere that we cone into a 3-disk D_{ij} . For each ij , we attach the 3-disk D_{ij} to T'_1 over $D_i \cup A_{ij} \cup D_j$ to form the closed solid torus T' .

By construction, $\partial T' = \partial T$, so T and T' are complementary. Moreover, $\gamma_i \subset \partial T'$ explicitly bounds a triangulated disk in T' , thus the γ_i are meridians of T' . We glue T to T' over their shared boundary to form a 3-sphere, then cone that 3-sphere into a 4-disk with an explicit 2-handle structure. We find a 2-handle for each face block analogue by iterating Algorithm 3 over the face block analogues of $M_1 \subset \partial W$, and attach these 2-handles to W , forming W' .

Data: A pair (T, Γ) where T is a closed solid torus triangulation and Γ is a collection of disjoint parallel triangulated longitudes in ∂T

Result: A 4-disk H_T^2 such that ∂H_T^2 is a triangulated 3-sphere with genus 1 Heegard splitting over ∂T and such that $\gamma_i \in \Gamma$ bounds a triangulated disk in $\partial H_T^2 \setminus \text{int}(T)$ for each i

```

1 begin
2   First, we construct a complementary solid torus  $T'$  with  $\partial T = \partial T'$ 
3    $T'_0 = \partial T$ 
4   foreach  $\gamma_i \in \Gamma$  do
5      $D_i = C(\gamma_i)$ , the cone of  $\gamma_i$ 
6   end
7    $T'_1 = T'_0 \cup \{D_i\} / \sim$ , where  $\sim$  is induced by  $\partial D_i = \gamma_i \xrightarrow{\iota} \gamma_i \subset T'_0$ 
8   foreach adjacent pair of longitudes  $\gamma_i, \gamma_j$  from  $\Gamma$  do
9      $A_{ij}$  = the annulus in  $T'_1$  bounded by  $\gamma_i$  and  $\gamma_j$ 
10     $S_{ij}$  = the triangulated 2-sphere in  $T'_1$  bounded by  $D_i \cup A_{ij} \cup D_j$ 
11     $D_{ij} = C(S_{ij})$ , the cone of  $S_{ij}$ 
12  end
13   $T' = T'_1 \cup \{D_{ij}\} / \sim$ , where  $\sim$  is induced by  $\partial D_{ij} = S_{ij} \xrightarrow{\iota} S_{ij} \subset T'_1$ 
14   $S_T^3 = T \cup T' / \sim$ , where  $\sim$  is induced by  $\partial T \xrightarrow{\iota} \partial T'$ 
15   $H_T^2 = C(S_T^3)$ , the cone of  $S_T^3$ 
16 end

```

Algorithm 3: Constructing a 2-handle

Let \mathfrak{B} be the collection of face block analogues of $M_1 \subset \partial W$. Iterating Algorithm 3 over \mathfrak{B} yields a collection of 4-dimensional 2-handles $\{H_B^2\}_{B \in \mathfrak{B}}$. The face block analogues in \mathfrak{B} are disjoint by construction, so we attach our 2-handles in any order. We form the 4-manifold triangulation W' from W as

$$W' = W \cup \{H_B^2\}_{B \in \mathfrak{B}} / \sim,$$

where \sim is defined by $b \sim \iota(b)$, ι the identity map $H_B^2 \supset B \xrightarrow{\iota} B \subset M_1$.

4.3.2 Attach 3–handles

We now have a triangulated 4–manifold with boundary components M_0 and the result of surgery on M_1 induced by 2–handle attachment. This surgery had the following effect on M_1 :

1. Each solid torus in the partition of M_1 induced by the projection from Section 4.1 is associated with a triangulated D^4 in Section 4.3.1.
2. For each (torus, 2–handle) pair (T, H^2) , the boundary of H^2 contains T and $T^* = H^2 \setminus \text{int}(T)$ is another solid torus whose boundary triangulation is identical to that of T .
3. Thus the effect of surgery on M_1 is of replacing each T with T^* over their shared boundary.

Chapter 5

Conclusion

Bibliography

- [1] Harold Levine. Elimination of cusps. *Topology*, 3(2):263–296, 1965.
- [2] Bjorn Poonen and Michael Rubinstein. The number of intersection points made by the diagonals of a regular polygon. *SIAM Journal on Discrete Mathematics*, (1) 11:135–156, 1998.
- [3] Osamu Saeki. *Topology of Singular Fibers of Differentiable Maps*. Lecture Notes in Mathematics 1854. Springer, 2004.
- [4] Saul Schleimer. Waldhausen’s theorem. *Geometry & Topology Monographs*, 12:299–317, 2007.
- [5] Shmuel Weinberger. *The topological classification of stratified spaces*. Chicago, 1994.